Journal of Nanofluids
Vol. 9, pp. 375–387, 2020
(www.aspbs.com/jon)

ARTICLE

Magnetohydrodynamics Williamson Fluid Comprising Gyrotactic Microorganisms Flows Through a Permeable Stretching Layer with Variable Fluid Properties

Amit Parmar[1,*], Rakesh Choudhary[2], and Krishna Agarwal[1]

[1]*Poornima University, Plot No. IS-2027-2031, Ramchandrapura P.O. Vidhani, Vatika Rd., Sitapura, Jaipur 303905, Rajasthan, India*
[2]*Bhartiya Skill Development University Jaipur, 302042, Rajasthan, India*

The present study shows the impacts of Williamson fluid with magnetohydrodynamics flow containing gyrotactic microorganisms under the variable fluid property past permeable stretching sheet. Variable Prandtl number, mass Schmidt number, and gyrotactic microorganisms Schmidt number were all considered. The momentum, energy, mass, and microorganism equations' governing PDEs are converted into nonlinear coupled ODEs and numerically solved with the bvp4c solver using suitable transformations. The main outcome of this study is that Williamson fluid parameter constantly decreases in velocity profile, however reverse effects can be shown in temperature profile. Also, *M* parameter and *Kp* parameter enhance the heat transfer rate, concentration rate and microorganisms boundary layer thickness but declines in momentum boundary layer thickness and velocity profile. The aim of this research is to see how velocity slide, temperature jump, concentration slip, and microorganism slip affect MHD Williamson fluid flow with gyrotactic microorganisms over a leaky surface embedded in spongy medium, with non-linear radiation and non-linear chemical reaction.

KEYWORDS: Williamson Fluid, Non-Linear Radiation, Microorganism, Slip Boundary Condition, Variable Prandtl Number, Variable Schmidt Number.

1. INTRODUCTION

The momentum and energy transfer of fluids plays important role in industry, research and engineering field. Non-Newtonian fluids has plays significance role in various manufacturing processes such as wire and fibre coating, extrusion of molten polymers through a slit die for the production of plastic sheets, paper production and processing of foodstuffs. Williamson fluid model describes the flow of shear thinning for non-Newtonian fluid it is a viscoelastic fluid.

As we know that viscoelastic fluid contains both viscous and elastic properties. Williamson explained the properties of pseudo-plastic materials and proposed a model of equations to explain this type of fluid flow. This model fits the experimental data of polymer solution and particle suspensions better than other models. So, for pseudo-plastic fluids, for which the apparent viscosity does not go to zero at infinity. Williamson fluid model has been studied by several researchers under various flow pattern, such as, Parmar[1–2] examined the non-Newtonian fluid and variable fluid property past a different surface such as a moving wedge and inclined porous stretching sheet with the convective boundary condition. Gorla et al.[3–5] investigated the analyzed of (Kn) chemical reaction and (R) nonlinear thermal radiation on MHD Williamson nanofluid fluid flow with melting, convective and slip boundary condition over a stretching/shrinking sheet embedded in a porous medium. Khan et al.[6] examined non-Newtonian Williamson fluid flow. Nadeem et al.[7–11] analyzed the Williamson fluid flow over a various surface conditions. Williamson[12] proposed pseudo plastic material flow. Dapra and Scarpi[13] looked into the possibility of pulsatile Williamson fluid movement in a rock fracture. Monica et al.[14] investigated radiative Williamson fluid movement over a stretching sheet. MHD Williamson nano fluid flow and heat transfer with viscous dissipation were investigated by Narayana et al.[15] Several researchers[16–24] investigated the non-Newtonian Williamson fluid flow for various boundary with various physical condition.

*Author to whom correspondence should be addressed.
Email: amit.198631@gmail.com
Received: 20 April 2021
Accepted: 10 May 2021

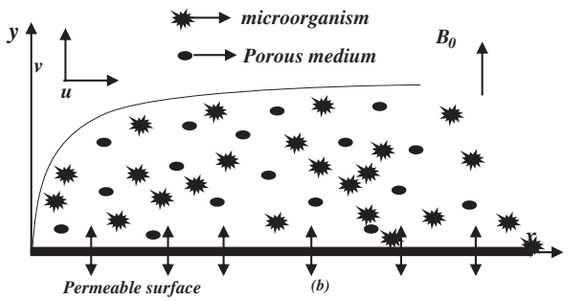

Fig. 1. Physical model and coordinate system of the problem.

Khan et al.[25] investigated the MHD gyrotactic microorganisms nano fluid with viscous dissipation and joule heating over a porous wedge. Avramenko and Kuznetsov[26] studied of gyrotactic microorganisms in superimposed fluid with porous layers. Khan et al.[27–28] proposed MHD gyrotactic microorganisms nanofluid over a convective heat, stretching sheet and vertical plate with Navier slip. Nield and Kuznetsov[29] examined gyrotactic microorganism's fluid flow. Several researchers have been done tremendous job on this topic.[30–59]

Even though substantial progress has been made in understanding flow phenomena over permeable stretching sheets, further work is needed to consider the outcomes of incorporating various non-Newtonian models and the formulation of correct methods of study for any body type with engineering implications. Theoretical research on the topic, on the other hand, is hindered by the complexity of the equations that describe the flows. The aim of this research is to see how velocity slide, temperature jump, concentration slip, and microorganism slip affect MHD Williamson fluid flow with gyrotactic microorganisms over a permeable surface embedded in porous medium, with non-linear radiation and non-linear chemical reaction.

2. MATHEMATICAL FORMULATION

MHD Williamson fluid flow over a permeable surface implanted in spongy medium in the presence of a magnetic field. A uniform magnetic field is applied at perpendicular to the fluid flow. On the flow field, no applied voltage or polarization voltage in imposed, therefore electric field $\vec{E} = 0$. Joule heating, viscous dissipation and Hall effects are neglected as Lorentz force depends only on magnetic field. Let surface is stretching is along the x axis with stretching velocity $u_w = Bx$. B is the positive constant. Following,[13] Williamson fluid modal is defined as

$$S = -pI + \tau \tag{1}$$

$$\tau = \left[\mu_\infty + \frac{(\mu_0 - \mu_\infty)}{1 - \Gamma\dot{\gamma}}\right] A_1 \tag{2}$$

where p is the pressure, I is the identity vector, τ is the extra stress tensor, μ_0, μ_∞ are the limiting viscosities at zero and infinite shear rates, $\Gamma > 0$ is a time constant, A_1 is the first Rivlin-Erickson tensor, and γ is defined as

$$\gamma = \sqrt{\frac{\pi}{2}} \quad \text{where } \pi = \text{trace}(A_1^2) \tag{3}$$

For $\mu_\infty = 0$ and $\Gamma\dot{\gamma} < 1$ thus the Eq. (2) can be rewritten as

$$\tau = \left[\frac{(\mu_0)}{1 - \Gamma\dot{\gamma}}\right] A_1 \tag{4}$$

Using binomial expansion on Eq. (4) we get

$$\tau = \mu_0\left[1 + \Gamma\dot{\gamma}\right] A_1 \tag{5}$$

The continuity, momentum, energy,mass and microorganism equations are given by Refs. [42–44]

$$\frac{\partial u}{\partial x} + \frac{\partial v}{\partial y} = 0 \tag{6}$$

$$u\frac{\partial u}{\partial x} + v\frac{\partial u}{\partial y} = \frac{1}{\rho_\infty}\frac{\partial}{\partial y}\left(\mu(T)\frac{\partial u}{\partial y}\right)\left(1 + \sqrt{2}\Gamma\frac{\partial u}{\partial y}\right) - \left(\frac{\sigma B_0^2}{\rho_\infty} + \frac{\mu(\mathrm{T})}{\rho_\infty k_p}\right)u \tag{7}$$

$$u\frac{\partial T}{\partial x} + v\frac{\partial T}{\partial y} = \frac{1}{\rho_\infty C_p}\frac{\partial}{\partial y}\left(k(T)\frac{\partial T}{\partial y}\right) - \frac{1}{\rho_\infty C_p}\frac{\partial q_r}{\partial y} \tag{8}$$

$$u\frac{\partial C}{\partial x} + v\frac{\partial C}{\partial y} = D_m\frac{\partial^2 C}{\partial y^2} - k_n(C - C_\infty)^n \tag{9}$$

$$u\frac{\partial N}{\partial x} + v\frac{\partial N}{\partial y} + \frac{b_c w_c}{(C_w - C_\infty)}\frac{\partial}{\partial y}\left(N\frac{\partial C}{\partial y}\right) = D_n\frac{\partial^2 N}{\partial y^2} \tag{10}$$

Where $u(x, y)$ and $v(x, y)$ are the horizontal and vertical fluid velocity components. T and T_∞ are temperature and ambient fluid temperature. $\mu(T) = \mu_\infty(1 + a(T - T_w))$: Temperature-dependent viscosity, μ_∞: ambient viscosity, $k(T) = k_\infty(1 + b(T - T_\infty))$: temperature dependent thermal conductivity, k_∞: ambient thermal conductivity, $\varepsilon = b(T_w - T_\infty)$: thermal conductivity variation parameter, $\delta = a(T_w - T_\infty)$: viscosity variation parameter,

Boundary Conditions[3, 41]

$$u = u_w + L_1\frac{\partial u}{\partial y} + L_2\frac{\partial^2 u}{\partial y^2}, \quad v = -v_w, \quad T = T_w + L_3\frac{\partial T}{\partial y}, \quad C = C_w + L_4\frac{\partial C}{\partial y}, \quad N = N_w + L_5\frac{\partial N}{\partial y} \quad \text{at} \quad y = 0$$
$$u \to 0, \quad T \to T_\infty, \quad C \to C_\infty, \quad N \to N_\infty \quad \text{at} \quad y \to \infty \tag{11}$$

v_w suction/injection velocity. Following Rosseland approximation q_r, the radiation heat flux is given

$$q_r = -\left(\frac{4\sigma}{3k^*}\right)\frac{\partial T^4}{\partial y} = -\left(\frac{16\sigma}{3k^*}\right)T^3\frac{\partial T}{\partial y} \text{ (Gorla et al.[5]).}$$

3. SOLUTION

We now introduce the following relations for u, v as

$$u = Bxf'(\eta), \quad v = -\sqrt{Bv_\infty} f(\eta), \quad \eta = y\sqrt{\frac{B}{v_\infty}},$$
$$\theta(\eta) = \frac{T - T_\infty}{T_w - T_\infty}, \quad \phi = \frac{C - C_\infty}{C_w - C_\infty} \quad \text{and} \quad N(\eta) = \frac{N - N_\infty}{N_w - N_\infty} \tag{12}$$

Equations (7)–(11) and using Eq. (12) thus reduces to the following non-dimensional form

$$(1 + We\, f'')\left(f'''(1 + \delta(1-\theta)) - \delta\theta' f''\right) - f'^2 + f''f - \left[M + K_p(1 + \delta(1-\theta))\right] f' = 0 \tag{13}$$

$$\theta''\left(1 + \frac{4}{3}R\left((\theta_w - 1)\theta + 1\right)^3 + \varepsilon\theta\right) + \varepsilon\theta'^2 + 4R(\theta_w - 1)\theta'^2\left((\theta_w - 1)\theta + 1\right)^2 + Pr_\infty(f\theta') = 0 \tag{14}$$

$$\phi'' - Sc_\infty(K_n\phi^n - f\phi') = 0 \tag{15}$$

$$\omega'' + Sn_\infty(f\omega' - Pe(\omega'\phi' + \phi''(\omega + \sigma))) = 0 \tag{16}$$

Variable Prandtl number and Variable Schmidt number of mass and Variable Schmidt number of gyrotactic microorganisms: The assumption of the constant Prandtl number inside the boundary layer when the viscosity and thermal conductivity are temperature dependent leads to unrealistic results.[30–32] Therefore, the Prandtl number related to the variable viscosity and variable thermal conductivity is defined as

$$Pr_v = \frac{\mu(T)\, C_p}{k(T)} = \frac{C_p \mu_\infty(1 + \delta(1-\theta))}{k_\infty(1 + \varepsilon\theta)} = \frac{Pr_\infty(1 + \delta(1-\theta))}{(1 + \varepsilon\theta)}$$

At the surface $\eta = 0$ of the porous stretching, this can be written as

$$Pr_w = \frac{Pr_\infty(1 + \delta)}{(1 + \varepsilon)}$$

It can be seen that for $\delta = 0, \varepsilon = 0$ the variable Prandtl number Pr_w is equal to the ambient Prandtl number Pr_∞. It is mention that $\eta \to \infty$, i.e., outside the boundary-layer, $\theta(\eta)$ becomes zero, therefore, $Pr_\infty = Pr_v$ regardless of the values of δ and ε.

If the viscosity of the fluid varies with the temperature, then the Schmidt number varies too. Therefore, the Schmidt number related to the variable viscosity is defined as

$$Sc_v = \frac{\mu(T)}{D_m\rho_\infty} = \frac{\mu_\infty(1 + \delta(1-\theta))}{D_m\rho_\infty} = Sc_\infty(1 + \delta(1-\theta))$$
$$Sc_N = \frac{\mu(T)}{D_N\rho_\infty} = \frac{\mu_\infty(1 + \delta(1-\theta))}{D_N\rho_\infty} = Sc_{N\infty}(1 + \delta(1-\theta))$$

At the surface $\eta = 0$ of the porous stretching, this can be written as

$$Sc_v = \frac{\mu(T)}{D_m\rho_\infty} = \frac{\mu_\infty(1 + \delta)}{D_m\rho_\infty} = Sc_\infty(1 + \delta)$$
$$Sc_N = \frac{\mu(T)}{D_N\rho_\infty} = \frac{\mu_\infty(1 + \delta)}{D_N\rho_\infty} = Sc_{N\infty}(1 + \delta)$$

it can be seen that for $\delta = 0, \varepsilon = 0$ the variable Prandtl number Sc_w, Sc_{wN} is equal to the ambient Schmidt number of mass and gyrotactic microorganisms $Sc_\infty, Sc_{\infty N}$. It is mention that $\eta \to \infty$, i.e., outside the boundary-layer, $\theta(\eta)$ becomes zero, therefore, $Sc_\infty, Sc_{\infty N} = Sc_v, Sc_{vN}$ regardless of the values of δ and ε.

The non-dimensional temperature Eqs. (14)–(16) can be expressed as

$$\theta''\left(1 + \frac{4}{3}R\left((\theta_w - 1)\theta + 1\right)^3 + \varepsilon\theta\right) + \varepsilon\theta'^2 + 4R(\theta_w - 1) \times \theta'^2\left((\theta_w - 1)\theta + 1\right)^2 + \frac{Pr_v(1 + \varepsilon\theta)}{(1 + \delta(1-\theta))}(f\theta') = 0 \tag{17}$$

$$\phi'' - \frac{Sc_v}{(1 + \delta(1-\theta))}(K_n\phi^n - f\phi') = 0 \tag{18}$$

$$\omega'' + \frac{Sn_v}{(1 + \delta(1-\theta))}(f\omega' - Pe(\omega'\phi' + \phi''(\omega + \sigma))) = 0 \tag{19}$$

Boundary conditions Eq. (11) reduces as:

$$\eta = 0: \quad f'(\eta) = 1 + Slip_1 f''(\eta) + \text{Slip}_2 f'''(\eta), \quad f(\eta) = S, \quad \theta(\eta) = 1 + \text{Slip}_T\theta'(\eta), \quad \phi(\eta) = 1 + \text{Slip}_C\phi'(\eta), \quad \omega(\eta) = 1 + \text{Slip}_C\omega'(\eta)$$
$$\eta \to \infty: \quad f'(\eta) \to 0, \quad \theta(\eta) \to 0, \quad \phi(\eta) \to 0, \quad \omega(\eta) \to 0 \tag{20}$$

Where, $We = \gamma x\sqrt{(2B^3/\nu_\infty)}$; non-Newtonian Williamson parameter, $\text{Slip}_1 = L_1\sqrt{(B/\nu_\infty)}$; $\text{Slip}_2 = L_2(B/\nu_\infty)$ $\text{Slip}_T = L_3\sqrt{(B/\nu_\infty)}$, $\text{Slip}_C = L_4\sqrt{(B/\nu_\infty)}$, $Slip_N = L_5\sqrt{(B/\nu_\infty)}$: first and second order slip velocity parameter, slip temperature parameter, slip concentration parameter and slip microorganism parameter respectively, $R = (4\sigma T_\infty^3)/(k_\infty k*)$; Radiation parameter, $k*$; thermal radiation parameter, $M = (\sigma B_0^2)/(\rho_\infty B)$: Magnetic field parameter, $K_n = (k_n/b)(C_w - C_\infty)^{n-1}$: chemical reaction parameter, $\theta_w = (T_w/T_\infty)$: temperature difference

ARTICLE

parameter, k_∞: thermal conductivity $K_p = (\nu_\infty/(k_p b))$: porosity parameter, $Pe = (b_c w_c)/\nu_\infty$: bioconvection Péclet number, $\sigma = N_\infty/(N_w - N_\infty)$: bioconvection constant, $Sn_\infty = (\nu_\infty/D_n)$: ambient Schmidt number of microorganism, $Sc_\infty = (\nu_\infty/D_B)$: ambient Schmidt number of mass $Pr_\infty = (\mu_\infty/k_\infty)C_p$ ambient Prandtl number, f': velocity profile, θ: temperature profile, ϕ: concentration profile and ω microorganisms profiles.

The skin friction coefficient C_f, local Nusselt number Nu_x, local Sherwood number Sh and local density number of the motile microorganisms Nn_x are defined as

$$C_f = \frac{\tau_w}{\rho U_w^2}, \quad Nu_x = \frac{-xq_w}{(T_w - T_\infty)} \left.\frac{\partial T}{\partial y}\right|_{y=0},$$

$$Sh = \frac{xJ_w}{D_B(C_w - C_\infty)} \quad \text{and}$$

$$Nn_x = \frac{xq_n}{D_n(\mathrm{N}_w - N_\infty)} \tag{21}$$

where $\tau_w = \left[(\partial u/\partial y) + (\Gamma/2)\left((\partial u/\partial y)\right)^2\right]\Big|_{y=0}$, $q_w = -k_\infty(\partial T/\partial y) + (q_r)_w|_{y=0}$; $J_w = -D_B(\partial C/\partial y)_{y=0}$,

$$q_n = -D_n\left(\frac{\partial N}{\partial y}\right)_{y=0} \tag{22}$$

On substituting value from Eq. (21) into Eq. (22), we get the following dimensionless expressions for skin friction coefficient, local Nusselt number and local Sherwood number as given below:

$$c_f Re_x^{1/2} = \left(f'' + \frac{We}{2}f''^2\right)\Big|_{\eta=0} \tag{23}$$

$$NuRe_x^{-1/2} = -\left(1 + \frac{4R}{3}\theta_w^3\right)\theta'(0) \tag{24}$$

$$Sh/\sqrt{Re} = -\phi'(0) \tag{25}$$

$$Nn_x/\sqrt{Re} = -\omega'(0) \tag{26}$$

$Re = (xu_x)/\nu_\infty$: local Reynolds number.

4. RESULTS AND DISCUSSION

The fix value of physical parameters $S = 0.2$, $R = M = 1$, $Pr = 4$, $Sc_v = Sn_v = 2$, $Kp = Kn = 0.5$, $We = \mathrm{slip}_1 = 0.1$, $\mathrm{slip}_2 = 0.05$, $\mathrm{slip}_T = \mathrm{slip}_C = \mathrm{slip}_N = 0.1$, $\varepsilon = \delta = 0.2$; $\theta_w = 1.5$, $n = 2$, $Pe = 0.2$, $\sigma = 0.5$; and excluding the varied value of the particular graph with specific two boundary conditions such as permeable and melting surfaces. Several sets of numerical solutions have been carried out for different combinations of pertinent parameters namely, chemical reaction parameter (Kn), Williamson fluid parameter (We), radiation parameter (R), magnetic field parameter (M), and suction/injection parameter (S) etc.

Figures 2–5 present the effect of M on the f', θ, ϕ and ω profiles. It is observed from Figure 2 that the f'

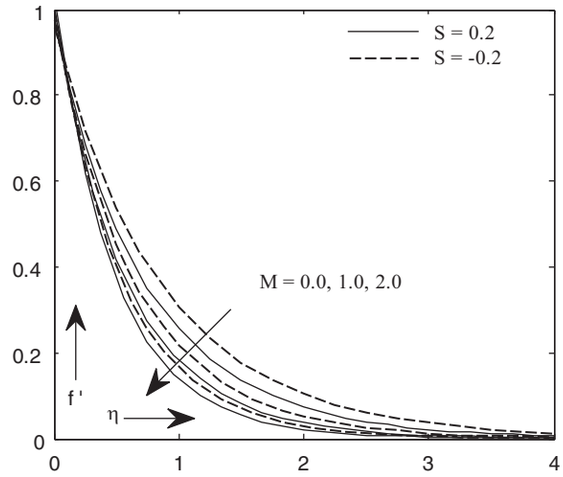

Fig. 2. Impact of M on f'.

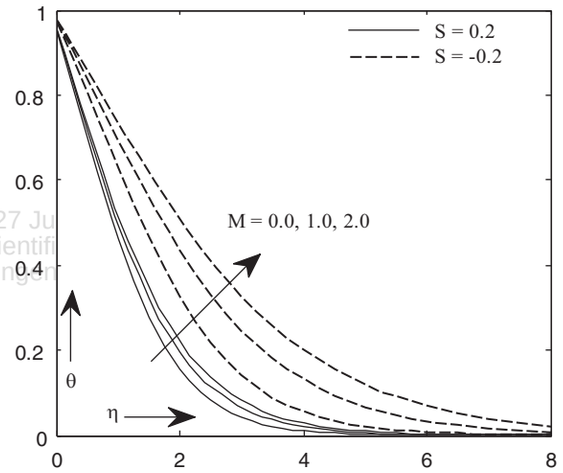

Fig. 3. Impact of M on θ.

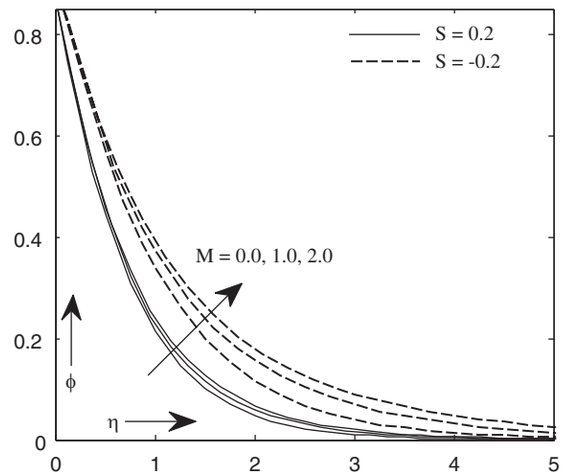

Fig. 4. Impact of M on ϕ.

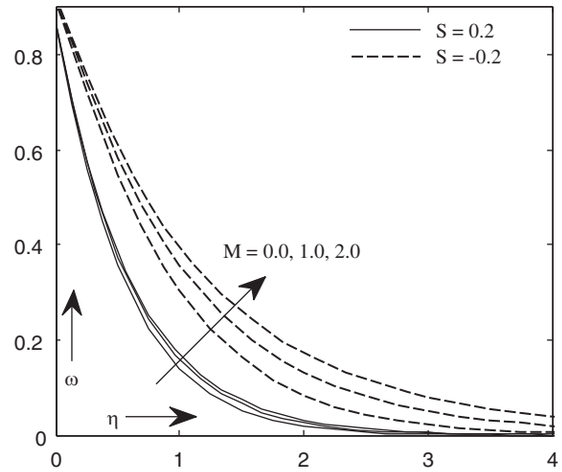

Fig. 5. Impact of M on ω.

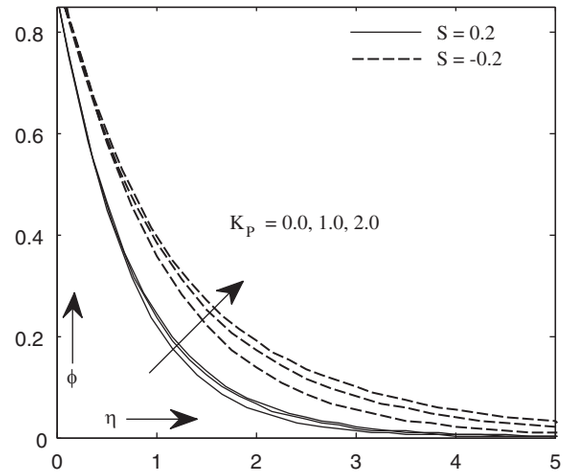

Fig. 8. Impact of Kp on ϕ.

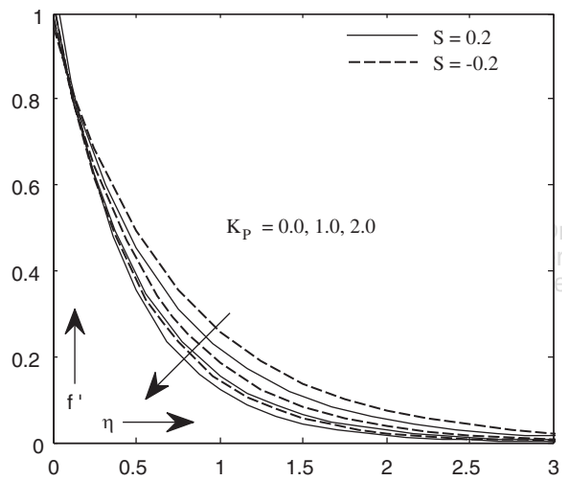

Fig. 6. Impact of Kp on f'.

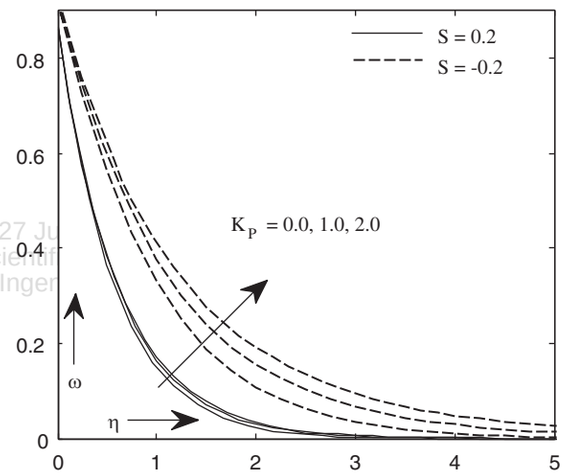

Fig. 9. Impact of Kp on ω.

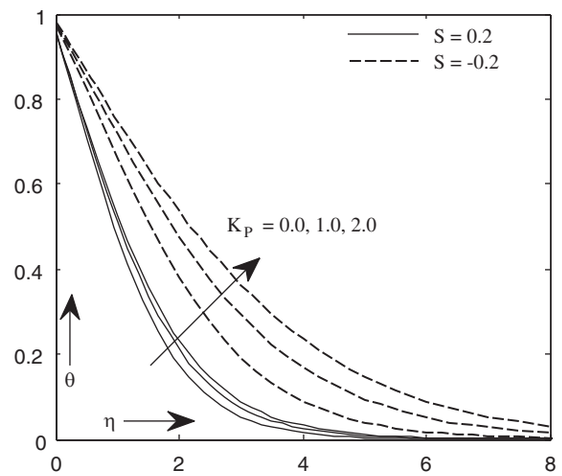

Fig. 7. Impact of Kp on θ.

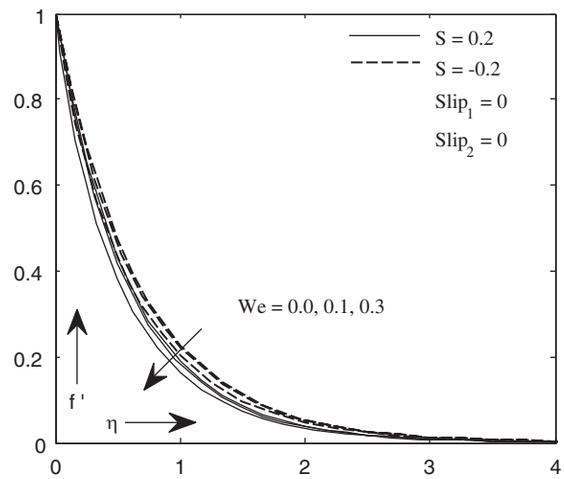

Fig. 10. Impact of We on f'.

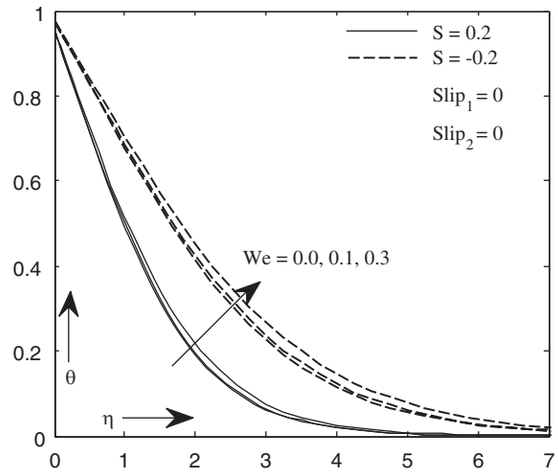

Fig. 11. Impact of *We* on θ.

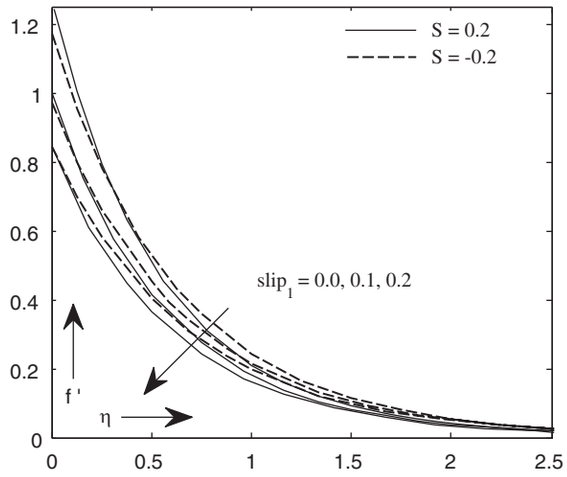

Fig. 14. Impact of slip_1 on f'

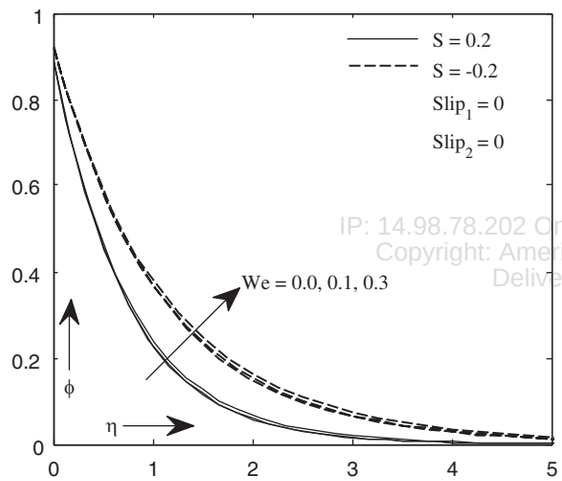

Fig. 12. Impact of *We* on ϕ.

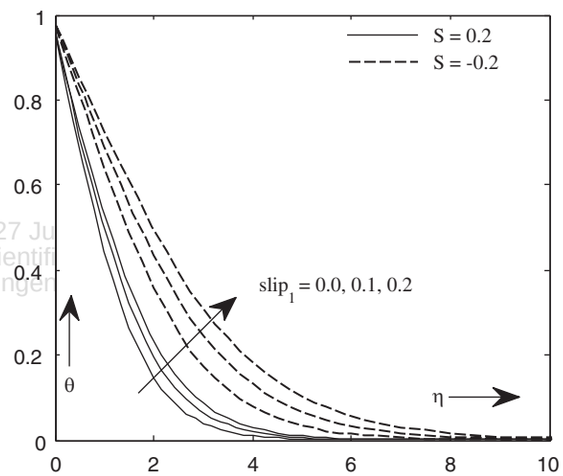

Fig. 15. Impact of slip_1 on θ.

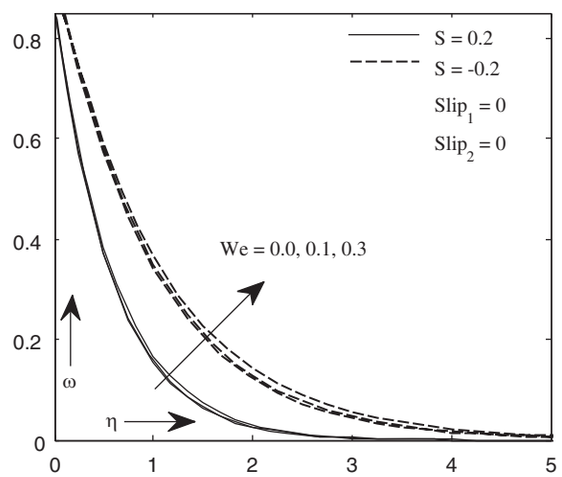

Fig. 13. Impact of *We* on ω.

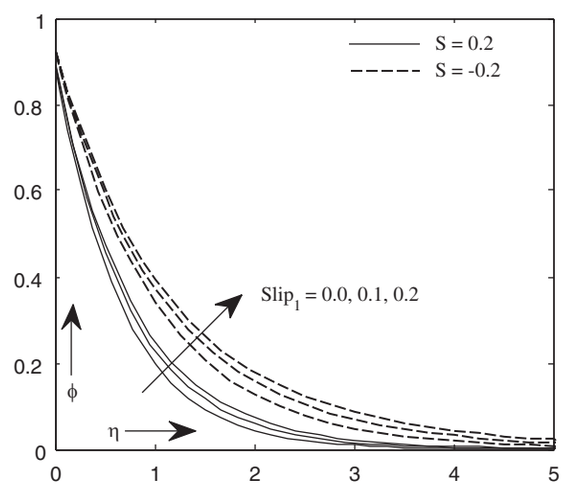

Fig. 16. Impact of slip_1 on ϕ.

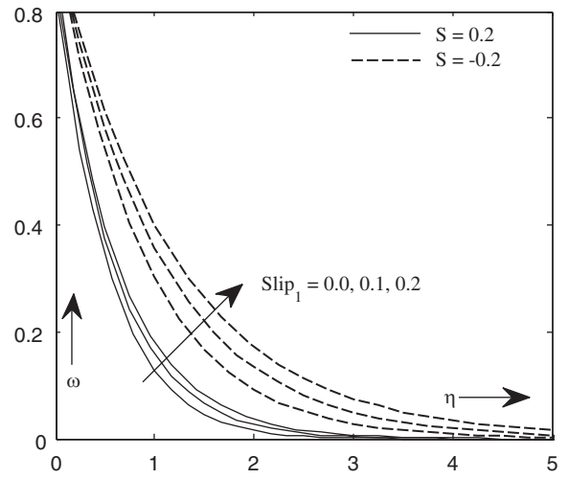

Fig. 17. Impact of slip$_1$ on ω.

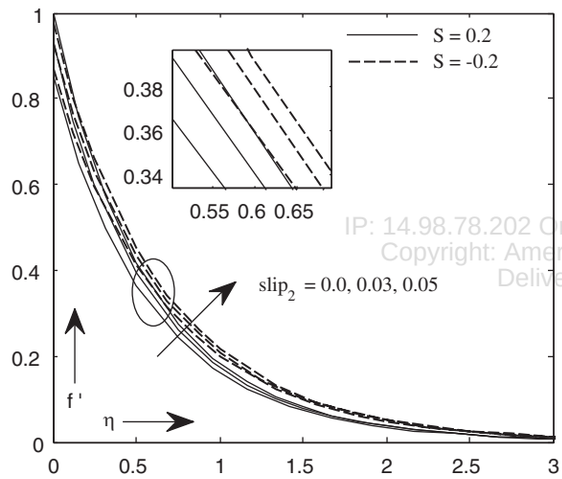

Fig. 18. Impact of slip$_2$ on f'.

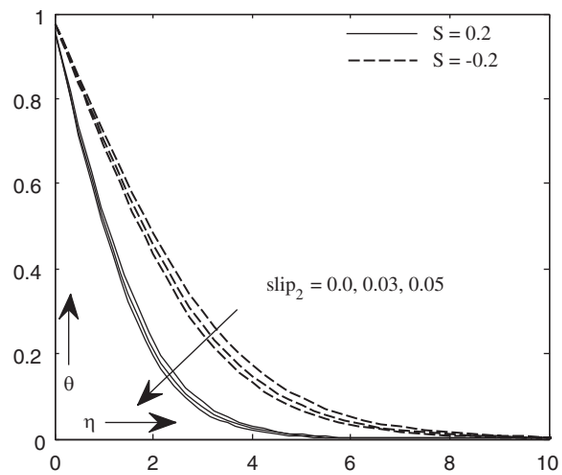

Fig. 19. Impact of slip$_2$ on θ.

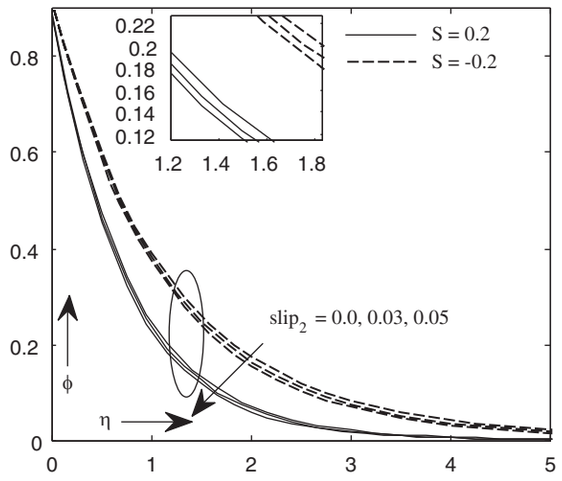

Fig. 20. Impact of $slip_2$ on ϕ.

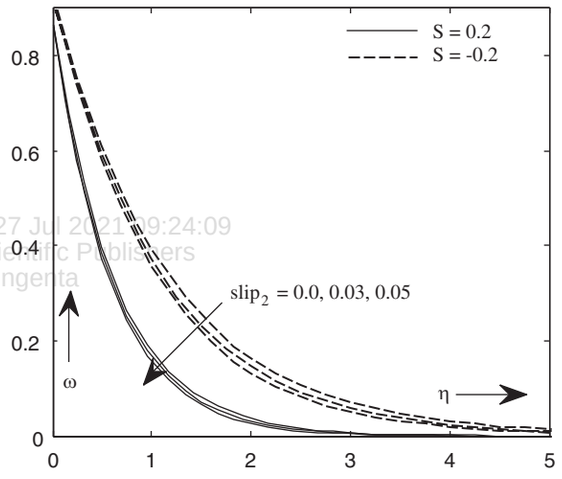

Fig. 21. Impact of slip$_2$ on ω.

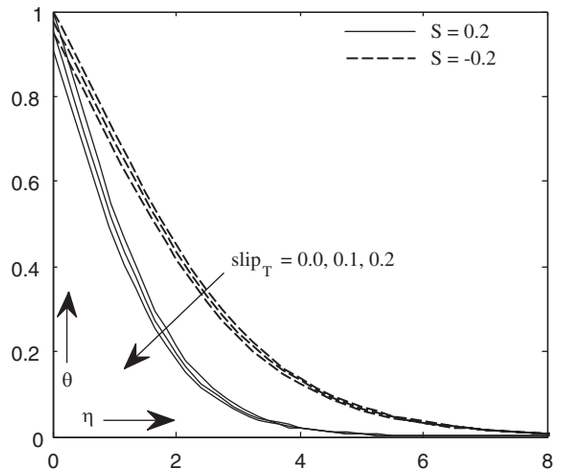

Fig. 22. Impact of slip$_T$ on θ.

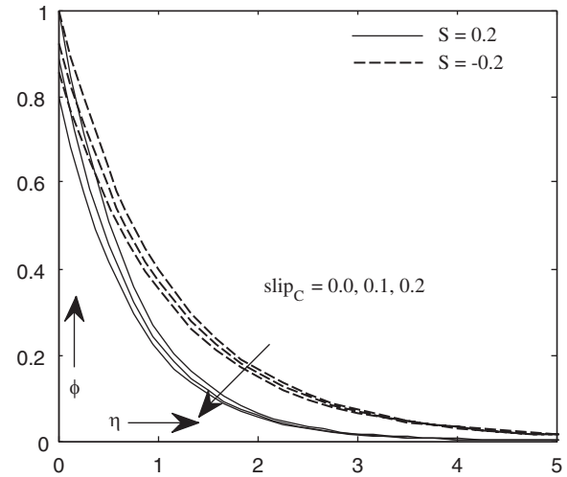

Fig. 23. Impact of slip$_C$ on ϕ.

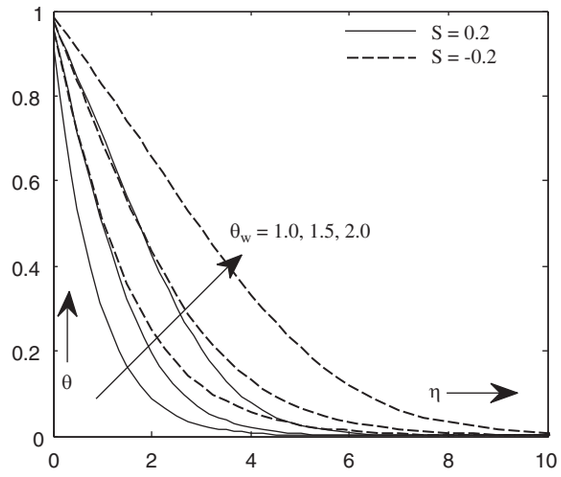

Fig. 26. Impact of θ_w on θ.

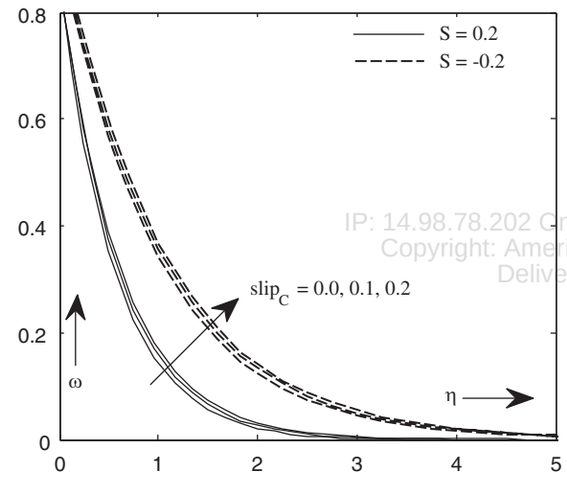

Fig. 24. Impact of slip$_C$ on ω.

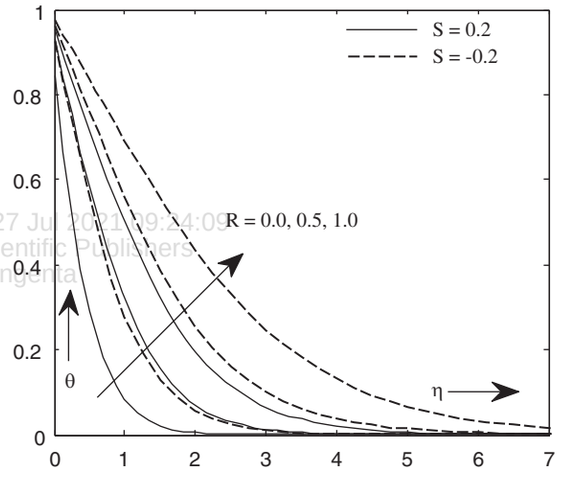

Fig. 27. Impact of R on θ.

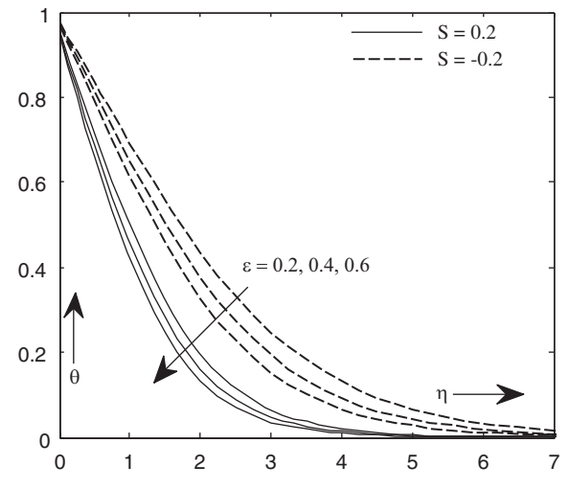

Fig. 25. Impact of ε on θ.

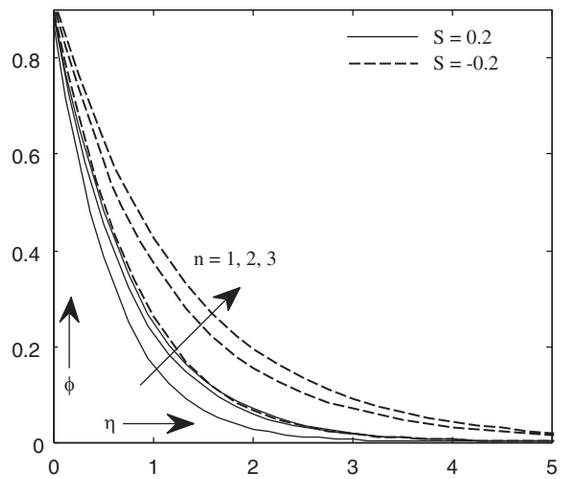

Fig. 28. Impact of n on ϕ.

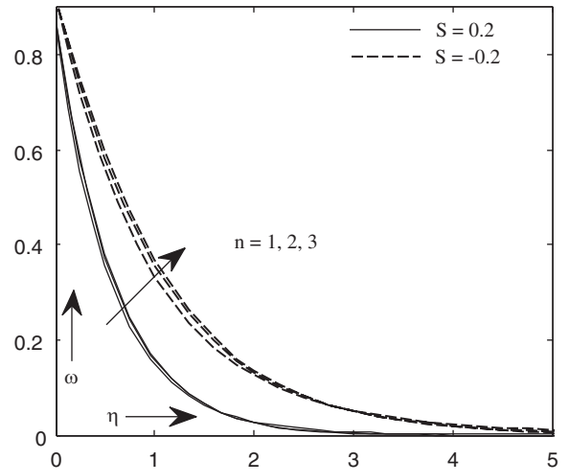

Fig. 29. Impact of n on ω.

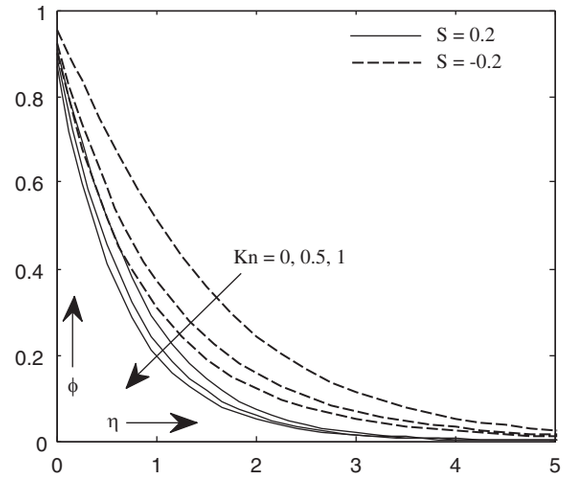

Fig. 32. Impact of Kn on ϕ.

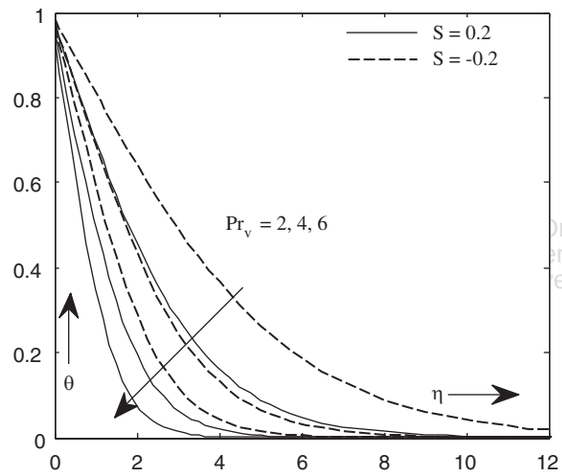

Fig. 30. Impact of Pr_V on θ.

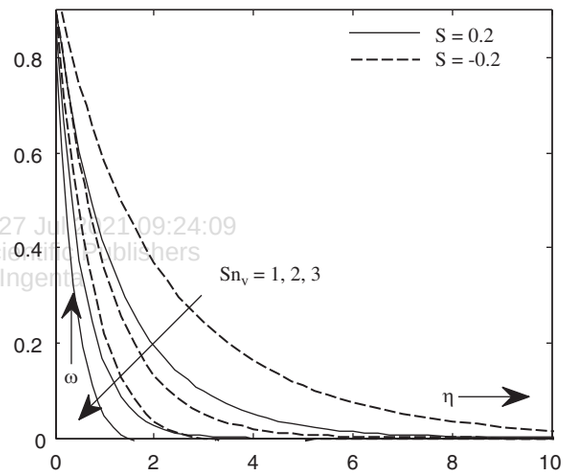

Fig. 33. Impact of Sn_V on ω.

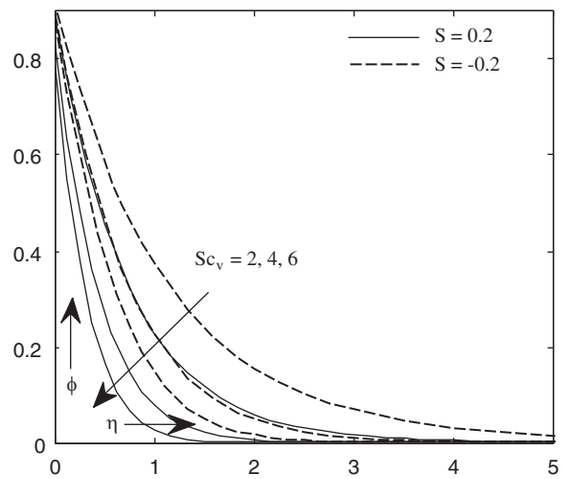

Fig. 31. Impact of Sn_V on ϕ.

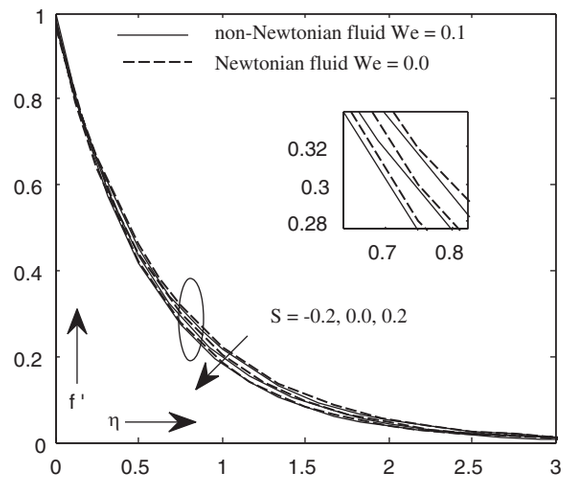

Fig. 34. Impact of S on f'.

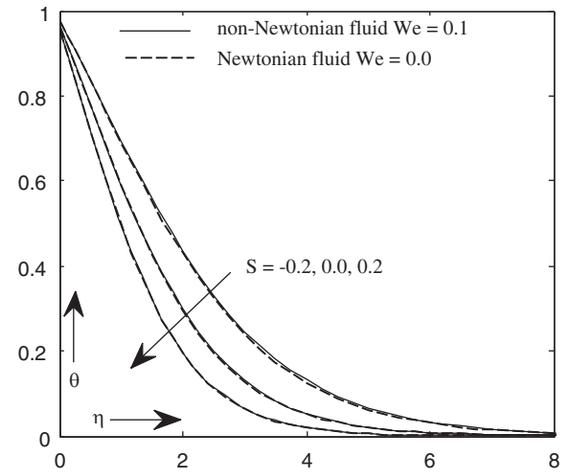

Fig. 35. Impact of S on θ.

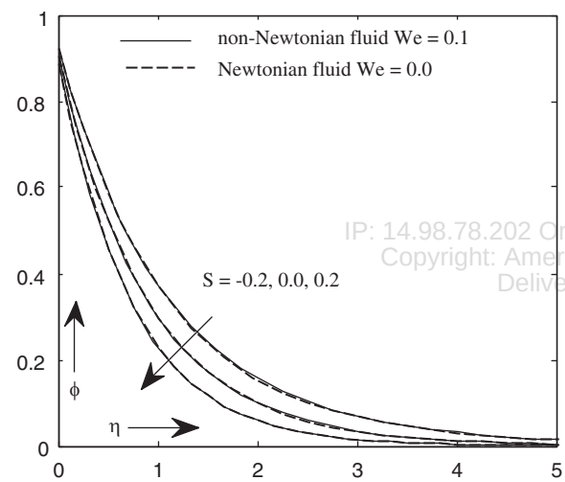

Fig. 36. Impact of S on ϕ.

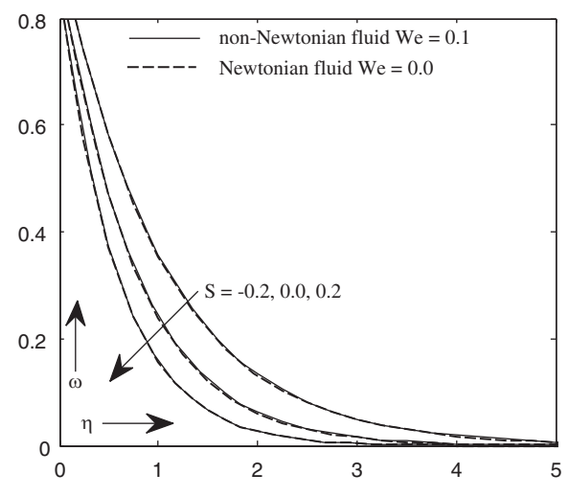

Fig. 37. Impact of S on ω.

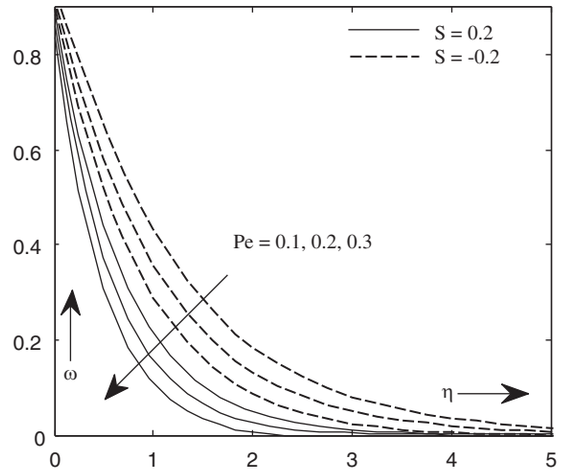

Fig. 38. Impact of Me on ω.

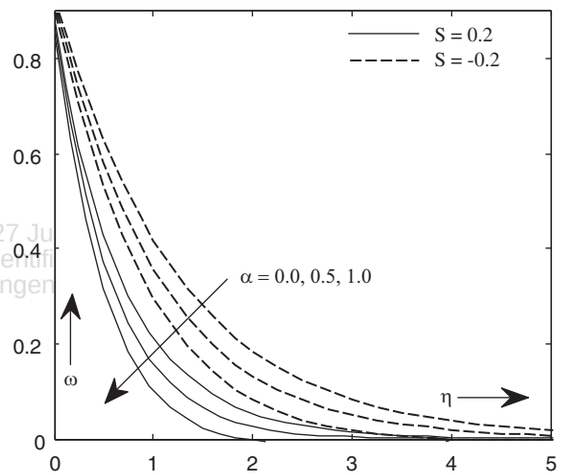

Fig. 39. Impact of σ on ω.

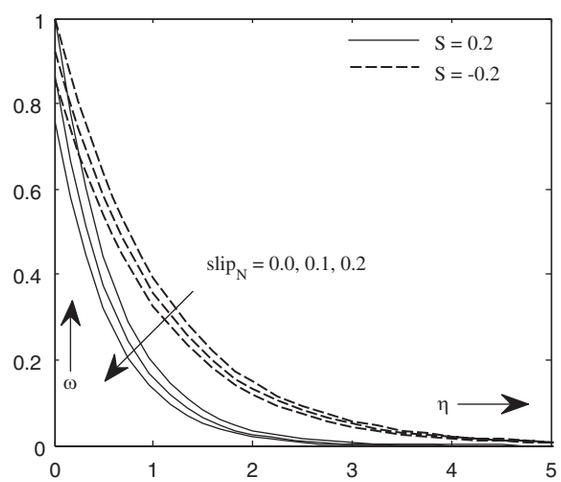

Fig. 40. Impact of slip_N on ω.

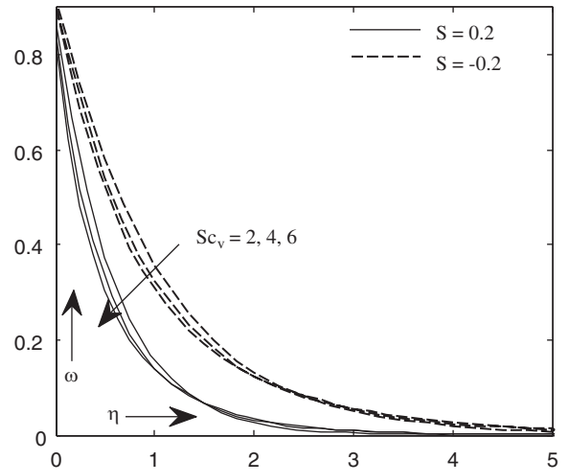

Fig. 41. Impact of Sc_V on ω.

decreases with an increase in M and Figures 3–5 the θ, ϕ and ω profiles are increasing with an increase in M. Physically, a M has the tendency to produce a drag-like force known as the Lorentz force which acts against flow, causing a flow retardation and enhancement thermal energy and concentration.

Figures 6–9 are displayed to analyze the impact of Kp parameter on the f', θ, ϕ and ω profiles. It is noticed that the f' profile suppress and θ, ϕ and ω profiles increase when Kp is increased. From Figures 10–13 they are observed that for a non-Newtonian fluid the velocity as well as the boundary layer thickness decreases and θ, ϕ and ω profiles increase with the increase in We parameter. Clearly f' is an increasing function of slip$_1$ parameter while the θ, ϕ and ω profiles decrease as shown in Figures 14–17.

Figures 18–21 show the f', θ, ϕ and ω profiles against the similarity variable η for various values of second order velocity slip parameter (slip$_2$). We observe from these figures that the f' profile increases as well as θ, ϕ and ω profiles decrease as slip$_2$ parameter increases. Physically, when slip occurs, the slipping fluid shows a decrease in the surface skin-friction between the fluid and the surface because not all the pulling force of the surface can be transmitted to the fluid. So, increasing the value of velocity slip parameter will decrease the flow velocity in the region of the boundary layer. The variation of θ profile with respect to slip$_T$ parameter is presented in

Figure 22. This figure depicts that temperature decreases by increasing slip$_T$. We also noted that the increase of parameter β causes a decrease in boundary layer thickness. Figures 23–24 show the influence of (slip$_C$) on ϕ and ω profiles. Increases the slip$_C$, reduces the ϕ profile and exact reverse effect have been observed for the ω profile. The variation of θ profile with respect to ε parameter is presented in Figure 25. This figure depicts that temperature decreases by increasing ε. Figures 26–27 show the impact of θ_w and R parameters on θ profile. From these graphs, it is clear that the surface temperature increases with increases in the value of the θ_w and R parameter.

Figures 28–29 show the impact of n parameter on ϕ and ω profiles. Raising the value of n parameter, enhancements the ϕ and ω profiles. The variation of θ with respect to Pr_v parameter is presented in Figure 30. This figure depicts that θ suppresses by increasing Pr_v. Pr is that

Table I. The skin friction coefficient C_f, local Nusselt number Nu_x and local Sherwood number Sh are following physically parameter such as $S = 0.2$, $R = M = 1$, $Pr = 4$, $Sc_v = Sn_v = 2$, $Kp = Kn = 0.5$, $We = \text{slip}_1 = 0.1$, $\text{slip}_2 = 0.05$, $\text{slip}_T = \text{slip}_C = \text{slip}_N = 0.1$, $\varepsilon = \delta = 0.2$; $\theta_w = 1.5$, $n = 2$, $Pe = 0.2$, $\sigma = 0.5$.

M	Kp	We	ε	R	θ_w	Sc_v	$c_f Re_x^{1/2}$	$NuRe_x^{-1/2}$	$ShRe^{-1/2}$	$NuRe^{-1/2}$
0							−1.2834415	2.7610238	1.1658025	1.4167415
1							−1.6596773	2.5889580	1.1410189	1.3819899
2							−1.9966720	2.4782272	1.1258123	1.3597992
	0						−1.4577052	2.6643221	1.1521919	1.3980439
	1						−1.8401763	2.5248608	1.1336684	1.3719403
	2						−2.2320614	2.4546516	1.1265412	1.3622308
		0.0					−1.7034108	2.6140956	1.1464503	1.3905604
		0.1					−1.6511537	2.5837151	1.1411827	1.3825832
		0.3					−1.5144449	2.4987330	1.1259036	1.3588642
			0.2				−1.6514522	2.5838886	1.1412205	1.3826431
			0.4				−1.6540333	2.8726282	1.1383227	1.3768860
			0.6				−1.6564327	3.1468021	1.1357570	1.3717572
				0.0			−1.6928350	1.5445913	1.1089943	1.3164314
				0.5			−1.6630546	2.2998581	1.1288966	1.3579953
				1.0			−1.6514522	2.5838886	1.1412205	1.3826431
					1		−1.6685279	2.0667838	1.1262763	1.3520772
					1.5		−1.6514522	2.5838886	1.1412205	1.3826431
					2.0		−1.6399010	2.9197329	1.1559544	1.4113958
						2	−1.6514522	2.5838886	1.1412205	1.3826431
						4	−1.6514446	2.5838845	1.7102671	1.6256371
						6	−1.6514434	2.5838835	2.1424636	1.8102435

ARTICLE

Table II. Comparison of $-\theta'(0)$ for different values Pr in the absence of the parameters $S = M = R = Kp = We = \text{slip}_1 = \text{slip}_2 = \text{slip}_T = \varepsilon = \delta = 0.0$; $\theta_w = 1$.

Pr	HAM method Nadeem and Hussain[34]	Gorla and Sidawi[35]	FEM method Goyal and Bhargava[36]	RKF45 method Gorla et al.[5]	bvp4c present study
0.2	0.169	0.1691	0.1691	0.170259788	0.172348764
0.7	0.454	0.5349	0.4539	0.454447258	0.453917857
2	0.911	0.9114	0.9113	0.911352755	0.911361492
7	–	1.8905	1.8954	1.895400395	1.895412536
20	–	3.3539	3.3539	3.353901838	3.353933867

Table III. Comparison of $-f''(0)$ for different values M in the absence of the parameters $S = R = Kp = We = \text{slip}_1 = \text{slip}_2 = \text{slip}_T = \varepsilon = \delta = 0.0$; $\theta_w = 1$, $Pr = 0.72$.

M	Andersson et al.[37]	Prasad et al.[38]	Mukhopadhyay et al.[39]	Palani et al.[40]	Present study
0.0	1.000000	1.000174	1.000173	1.00000	1.000000000
0.5	1.224900	1.224753	1.224753	1.224745	1.224744871
1	1.414000	1.414449	1.414450	1.414214	1.414213562
1.5	1.581000	1.581139	1.581140	1.581139	1.581138830
2	1.732000	1.732203	1.732203	1.732051	1.732050808

the ratio of momentum to thermal diffusivity. Fluids with a lower Prandtl number (and thicker thermal physical phenomenon structures) can disperse heat from the sheet faster than fluids with a better Prandtl number (thinner boundary layers). The Prandtl number are often wont to maximize the speed of cooling in conducting flows.

Figures 31–32 show the influence of Kn and Sc_v on ϕ profile. Increasing the value of Kn and Sc_v, reduce the ϕ profile. Kn increases the rate of interfacial mass transfer. Chemical reaction parameter reduces the local concentration, thus increases its concentration gradient and its flux. Physically, it is due to the fact that Sc_v is the ratio of momentum to mass diffusivities which means that when Sc_v increases, mass diffusivity decreases and there is a reduction in concentration.

Figure 33 shows the influence of Sn_v number on microorganisms profile. This figure depicts that ω profile decreases by increasing Sn_v. Figures 34–37 show the f', θ, ϕ and ω profiles against the similarity variable η for various values of S parameter. We observe f', θ, ϕ and ω profiles decrease as S increases.

Figures 38–41 show the ω profile against the similarity variable η for various values of following parameters such as Pé, σ, slip_N and Sc_v. We are noted that the ω profile decreases Pé, σ, slip_N and Sc_v increases.

Table I shows the variation of $C_f Re_x^{1/2}$, $NuRe_x^{-1/2}$, $Sh\,Re^{-1/2}$ and $Nn\,Re^{-1/2}$ for various value of physical parameters. It is observed that as coefficient of skin friction oscillates, local Nusselt number, local Sherwood number and local density number of the motile microorganisms decreases as We and Kp increase. An increment in radiation parameter (R) shows increment in $NuRe_x^{-1/2}$ and decrement in $Sh\,Re^{-1/2}$ and $Nn\,Re^{-1/2}$. Tables II and III are displayed to analyze the comparison of the present analytical results with the existing numerical solutions for the following researchers such as Golra et al.,[5] Nadeem and Hussain[34] Gorla and Sidawi[35] Goyal and Bhargava[36] Andersson et al.,[37] Prasad et al.,[38] Mukhopadhyay et al.[39] and Palani et al.[40] Under some special conditions, present results have an excellent agreement with the existed results. This shows the validity of the present results along with the accuracy of the numerical technique we used in this study.

5. CONCLUSION

We have investigated the effect of first and second order velocity slip, temperature slip, concentration jump and microorganisms jump on MHD Williamson fluid flow over a permeable surface embedded in porous medium with non-linear radiation and non-linear chemical reaction. The effects of various parameters on velocity, temperature, concentration and microorganisms profile can be summarized as follows:

- M parameter, Kp parameter, We parameter, slip_1 parameter has propensity to rises the thermal heat transfer rate, concentration rate and microorganisms boundary layer thickness and inverse impact show on momentum boundary layer thickness and velocity profile.
- Kp parameter and We parameter increases, coefficient of skin friction oscillates, local Nusselt number, local Sherwood number and local density number of the motile microorganisms decreases.
- An increment in radiation parameter (R) shows an increment in local Nusselt number $NuRe_x^{-1/2}$ and decrement in local Sherwood number $Sh\,Re^{-1/2}$ and local density number of the motile microorganisms $Nn\,Re^{-1/2}$.

Conflict of Interest

The authors declare that there is no conflict of interests regarding the publication of this paper.

References and Notes

1. A. Parmar, *Int. J. Appl. Comput. Math.* 3, 611 **(2017)**.
2. A. Parmar, *Int. J. Appl. Comput. Math.* 3, 859 **(2017)**.
3. R. S. R. Gorla, M. R. Krishnamurthya, K. B. C. Prasann, and B. J. Gireesha, *An International Journal, Engineering Science and Technology* 19, 53 **(2016)**.
4. R. S. R. Gorla and B. J. Gireesha, *Heat Mass Transfer* 52, 1153 **(2016)**.
5. R. S. R. Gorla, K. B. C. Prasanna, B. J. Gireesh, and M. R. Krishnamurthy, *J. Aerosp. Eng.* 29, 04016019 **(2016)**.
6. N. Alam, H. Khan, and A. Khan, *Nonlinear Eng.* 3, 107 **(2014)**.
7. S. Nadeem, S. T. Hussain, and C. Lee, *Braz. J. Chem. Eng.* 30, 619 **(2013)**.
8. S. Nadeem and S. T. Hussain, *Appl. Math. Mech. Engl. Ed.* 35, 489 **(2014)**.
9. S. Nadeem and N. S. Akbar, *Int. J. Num. Methods Fluids* 66, 212 **(2010)**.
10. S. Nadeem and S. T. Hussain, *Appl. Nanosci.* 4, 1005 **(2014)**.
11. S. Nadeem and S. T. Hussain, *J. Appl. Fluid Mech.* 9, 729 **(2016)**.
12. R. V. Williamson, *Ind. Eng. Chem.* 21, 1108 **(1929)**.
13. I. Dapra and G. Scarpi, *Int. J. Rock Mech. Min. Sci.* 44, 271 **(2007)**.
14. M. Monica, J. Sucharitha, and C. K. Kumar, *American Chemical Science Journal* 13, 1 **(2016)**.
15. K. L. Narayana, K. Gangadhar, and M. J. Subhakar, *IOSR J. of Math (IOSR-JM)* 11, 4 **(2015)**.
16. N. A. Khan, S. Khan, and F. Riaz, *Math. Sci. Lett.* 3, 199 **(2014)**.
17. M. Y. Malik and T. S. Uddin, *International Journal of Nonlinear Sciences and Numerical Simulation* 16, 161 **(2015)**.
18. R. M. Darji and M. G. Timol, *Int. J. Adv. Appl. Math. and Mech.* 1, 10 **(2014)**.
19. B. Jyothi and P. K. Rao, *J. Math. Comp. Sci.* 3, 1306 **(2013)**.
20. B. A. Kumari, K. R. Prasad, and K. Kavitha, *Advances in Applied Science Research* 3, 2492 **(2012)**.
21. M. Kothandapania and J. Prakash, *International Journal of Heat and Mass Transfer* 81, 234 **(2015)**.
22. S. Jain and R. Choudhary, *Global and Stochastic Analysis Special Issue: 25th International Conference of Forum for Interdisciplinary Mathematics* SI: 75–84 **(2017)**.
23. S. Jain and R. Choudhary, *Procedia Engineering* 127, 1203 **(2015)**.
24. S. Jain and A. Parmar, Comparative study of flow and heat transfer behaviour of Newtonian and non-Newtonian fluids over a permeable stretching surface, *Global and Stochastic Analysis Special Issue: 25th International Conference of Forum for Interdisciplinary Mathematics*, SI: 41–50 **(2017)**.
25. U. Khan, N. Ahmed, and S. T. Mohyud Din, *Springer Plus* 5, 2043 **(2016)**.
26. A. A. Avramenko and A. V. Kuznetsov, *Int. Commun. Heat Mass Transf.* 31, 1057 **(2004)**.
27. W. A. Khan and O. D. Makinde, *Int. J. Therm. Sci.* 81, 118 **(2014)**.
28. W. A. Khan, O. D. Makinde, and Z. H. Khan, *Int. J. Heat Mass Transf.* 74, 285 **(2014)**.
29. D. A. Nield and A. V. Kuznetsov, *Int. J. Therm. Sci.* 45, 990 **(2006)**.
30. M. S. Alama, M. Asiya, M. M. Rahman, and K. Vajravelu, *International Journal of Mechanical Sciences* 105, 191 **(2016)**.
31. M. M. Rahman, M. A. Rahman, M. A. Samad, and M. S. Alam, *Int. J. Thermophys.* 30, 1649 **(2009)**.
32. M. M. Rahman and I. A. Eltayeb, *Int. J. Therm. Sci.* 50, 468 **(2011)**.
33. M. M. Rahman, *Can. J. Chem. Eng.* 90, 1631 **(2012)**.
34. S. Nadeem and S. T. Hussain, *Appl. Nanosci.* 4, 1005 **(2013)**.
35. R. S. R. Gorla and I. Sidawi, *Appl. Sci. Res.* 52, 247 **(1994)**.
36. M. Goyal and R. Bhargava, *Appl. Nanosci.* 4, 761 **(2014)**.
37. H. I. Andersson, O. R. Hansen, and B. Holmedal, *Int. J. Heat Mass Transfer* 37, 659 **(1994)**.
38. K. V. Prasad, A. Sujatha, K. Vajravelu, and I. Pop, *Meccanica* 47, 1425 **(2012)**.
39. S. Mukhopadhyay, A. M. Golam, and A. P. Wazed, *Chin. Phys. B* 22, 124701 **(2013)**.
40. S. Palani, B. R. Kumar, and P. K. Kameswaran, *Ain Shams Engineering Journal* 7, 399 **(2016)**.
41. A. M. Megahed, *Eur. Phys. J. Plus* 130, 81 **(2015)**.
42. M. Waqas, T. Hayat, M. I. Khan, and A. Alsaedi, *Int. J. Mechanical Sci.* 131–132, 426 **(2017)**.
43. M. Waqas, T. Hayat, S. A. Shehzad, and A. Alsaedi, *Physica B: Condensed Matter* 529, 33 **(2018)**.
44. F. Naseem, A. Shafiq, L. Zhao, and A. Naseem, *Aip Advances* 7, 065013 **(2017)**.
45. M. V. Krishna, M. G. Reddy, and A. J. Chamkha, *Int. Jour. of Fluid Mech. Res.* 45, 1 **(2019)**.
46. M. Veera Krishna, *International Communications in Heat and Mass Transfer* 119, 104927 **(2020)**.
47. M. V. Krishna, M. G. Reddy, and A. J. Chamkha, *Journal of Porous Media* 24, 81 **(2021)**.
48. B. H. Babu, P. S. Rao, and S. V. Krishna, *Numer Methods Partial Differential Eq.* 50, 1776 **(2020)**.
49. M. V. Krishna and A. J. Chamkha, *International Communications in Heat and Mass Transfer* 113, 104494 **(2020)**.
50. M. V. Krishna and A. J. Chamkha, *Results in Physics* 15, 102652, **(2019)**.
51. M. V. Krishna, B. V. Swarnalathamma, and A. J. Chamkha, *Journal of Ocean Engineering and Science* 4, 263 **(2019)**.
52. M. V. Krishna and A. J. Chamkha, *Journal of Porous Media* 22, 209 **(2019)**.
53. M. V. Krishna and A. J. Chamkha, *Journal of Egyptian Mathematical Society* 28, 1 **(2020)**.
54. M. V. Krishna and A. J. Chamkha, *Ain Shams Engineering Journal* 11, 1 **(2020)**.
55. M. V. Krishna, N. A. Ahamad, and A. J. Chamkha, *Ain Shams Engineering Journal* 11, 1 **(2021)**.
56. M. V. Krishna, N. A. Ahamad, and A. J. Chamkha, *Alexandria Engineering Journal* 60, 845 **(2021)**.
57. M. V. Krishna and B. V. Swarnalathamma, *AIP Conference Proceedings* 1728, 020603 **(2016)**.
58. M. V. Krishna and A. J. Chamkha, *Special Topics and Reviews in Porous media: An International Journal* 10, 245 **(2019)**.
59. M. V. Krishna and A. J. Chamkha, *AIP Conference Proceedings* 1728, 020461 **(2016)**.